Theoretical Calculations on the Torsion Potential of Peroxynitrite Anion in Aqueous Solution

Peter I. Nagy*

Department of Medicinal and Biological Chemistry, The University of Toledo, Toledo, Ohio 43606-3390

Received: September 6, 2001; In Final Form: December 21, 2001

Solvent effects have been calculated on the torsion potential of the peroxynitrite anion ($ONOO^-$) in aqueous solution, using the continuum solvent SCI−PCM method at the B3LYP/6-311+G* level, and by a combined (ab initio or DFT)/Monte Carlo simulation method at the MP2 and B3LYP levels using the 6-311+G* basis set. On the basis of the SCI−PCM calculations, the relative internal energy hardly changes for the cis and trans conformers upon solvation, but the difference in the solute−solvent interaction energy raises the free energy of the trans conformer relative to the cis to 4.3 kcal/mol, as compared to the gas-phase value of 3.1 kcal/mol at $T = 298.15$ K. Geometry distortion upon solvation is small, and subsequent changes in the relative thermal corrections for the different conformers are also small in general. B3LYP/Monte Carlo calculations at $T = 310$ K result in a decrease of the relative trans free energy to 1.8−2.5 kcal/mol when changes in the geometry upon solvation were considered, and the atomic charges were fit to the correlated charge distribution. All these results are in basic accord with the interpretation of the experimental in-solution Raman spectrum of $ONOO^-$, in favor of the cis form by Tsai et al. (*J. Am. Chem. Soc.* **1994**, *116*, 4115). The calculations, however, call the attention to the different trend of the solvent effect on the cis−trans free energy separation for peroxynitirite anion, when using the SCI−PCM and the Monte Carlo methods, and calculating the internal energy at the B3LYP/6-311+G* level. Aqueous solvation was calculated as decreasing the free energy of the barrier by 1.8 kcal/mol with the continuum dielectric solvent model, whereas the barrier decreased by up to 7 kcal/mol on the basis of B3LYP/MC and MP2/MC calculations. Accordingly, the free energy of the barrier was predicted as 18−24 kcal/mol for peroxynitirite anion in aqueous solution. The present study suggests that on the basis of combined (ab initio or DFT)/Monte Carlo calculations, solute thermodynamics and solution structure can be characterized in accord with available experimental data, if the solute geometry is previously optimized using a continuum solvent method, the atomic charges are fitted to a correlated charge distribution, and thermal corrections are considered even from gas-phase calculations.

Introduction

Peroxynitrite, $O{=}N{-}O{-}O^-$ is a stable anion formed by the reaction of nitric oxide and the superoxide anion in a biological environment.[1] The reaction product has strong cellular toxicity in humans,[2] acting as an oxidant of sulfhydryl groups and thioethers, and nitrating and hydroxylating aromatic compounds. $ONOO^-$ inhibits, among others, manganese superoxide dismutase, cytosolic aconitase, and several enzymes in the mitochondrial respiratory chain.[2] $ONOO^-$ is a stable anion in basic solution, but the parent peroxynitrous acid, ONOOH has a lifetime of only about 3 s at neutral pH, and isomerizes to nitric acid.[3]

Because of their significant biological relevance, the $ONOO^-$ and ONOOH systems have drawn increasing theoretical interest recently. For a better understanding of their possible interactions in a biological medium, determination of their structures is important. The $ONOO^-$ system exhibits a quasi cis−trans isomerism (Scheme 1). The central N−O bond has some double bond character, and the question emerges as to whether the molecule exists in one of the planar forms ($O_1...O_4$ cis and trans), or whether the most stable conformer is a nonplanar form with $O{=}N{-}O{-}O^-$ torsion angle between 0° and 180°. There are two rotating bonds in the ONOOH acid, allowing even larger conformational freedom.

SCHEME 1

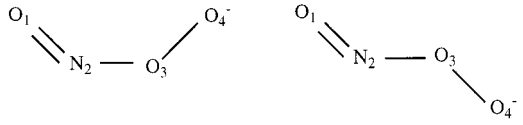

Tsai et al.[4] studied both molecules in the gas phase using ab initio quantum chemical methods up to the CCSD(T)/6-311+G(d) level, and DFT methods with the 6-311+G(d) basis set. The higher-level energy calculations for $ONOO^-$ predicted the preference of the cis form over the trans by 2−4 kcal/mol, and the cis barrier as high as 21−27 kcal/mol. The theoretically calculated vibrational frequencies were compared to the experimental Raman spectrum taken in aqueous alkaline solution.[5] Theoretical frequencies calculated for the $ONOO^-$ cis conformer at the CCSD level agreed well with the experimental values, except for the O−N−O−O torsion frequency.

Considering the effect of an aqueous environment, Tsai et al.[4] performed Becke3-LYP + SCI−PCM/6-311+G(d) calculations for the cis and trans $ONOO^-$. The solvent provided an additional 1 kcal/mol stabilization for the cis isomer. Ab initio studies of the peroxynitrite anion−water complexes[6] indicated the negatively charged oxygen atom as the strongest hydrogen

10.1021/jp013416n CCC: $22.00
Published on Web 02/27/2002

bonding site, both in the cis and the trans forms. Monohydrates having the water molecule at the O(=N) site are less stable than the $O^-\cdots HOH$ structure by about 6 kcal/mol. A conformational equilibrium study for the ONOOH system in aqueous solution was performed by Doclo and Rothlisberger.[7] The first-principle molecular dynamics study found increased preference for the O−N−O−O cis relative to the trans form in aqueous solution as compared to the gas phase.

In the solvent-effects study of Tsai et al.,[4] the SCI−PCM method[8a] using the dielectric continuum approach was applied. Their studies for the $ONOO^-$ mono- and dihydrates[6] indicated that the binding energy depends sensitively on the binding site. Thus, solvent effect calculations considering explicit water molecules could be useful.

The present paper has a double goal. The primary aim is to study the solvent effects on the torsion potential of the $ONOO^-$ anion. The small size of the solute, however, enables to target a second goal: a detailed investigation of several factors contributing to the solvent effects, including geometry change, polarization, change of vibrational frequencies, and thermal effects. Two different approaches, the continuum solvent approximation and Monte Carlo simulations with explicit water molecules, were applied and compared here. In the continuum solvent method the solute geometry was optimized in solution. Intramolecular and solute−solvent interaction energy components of the total energy were separated, and the solvation free energy contribution to the torsion potential was compared with the Monte Carlo relative solvation free energy values. Modification of the barrier height and the cis−trans free energy separation were determined. On the basis of Monte Carlo simulations, the hydrogen-bond pattern to the $ONOO^-$ anion was characterized in different conformations in relation to the solute geometry and charge parameters.

Theoretical Background and Calculations

In the continuum-dielectric solvent approximation the basic equation is[9]

$$(H_s^\circ + V_R)\,\Psi_s = E_s\,\Psi_s \tag{1}$$

where H_s° is the solute Hamiltonian at the geometry accepted for in solution, V_R is the solvent reaction potential term accounting for the solute−solvent stabilization energy and the reversible work required for polarizing the solvent. The solute is placed in a cavity created in the continuous solvent. Depending on the method by which the cavity has been created, there are several realizations of the polarizable continuum method (PCM).[9]

In the gas phase, the regular Schroedinger equation holds:

$$H_g^\circ\,\Psi_g = E_g\,\Psi_g \tag{2}$$

where H_g° is the Hamiltonian of the molecule at the optimized arrangement of nuclei in the gas phase.

Using the gas-phase and the in-solution solute Hamiltonians, which may differ only in the location of the nuclei, the following energies can be defined

$$E_s^\circ = \langle\Psi_s|\,H_s^\circ\,|\Psi_s\rangle \tag{3a}$$

$$E_g = \langle\Psi_g|\,H_g^\circ\,|\Psi_g\rangle \tag{3b}$$

$$E_{gs} = \langle\Psi_{gs}|\,H_s^\circ\,|\Psi_{gs}\rangle \tag{3c}$$

$$E_{susv} = \langle\Psi_s|\,V_R\,|\Psi_s\rangle \tag{3d}$$

E_{gs} is the energy of the isolated molecule in the gas phase at the geometry optimized in solution. E_{susv} accounts for the solute−solvent interaction energy calculated with the self-consistent V_R reaction-potential operator. Upon eqs 1, 3a, and 3d

$$E_s = E_s^\circ + E_{susv} \tag{3e}$$

The total free energy of the solute in solution, $G_{stot}(\tau)$, will be defined here for the PCM calculations as

$$G_{stot}(\tau) = G_{elst}(\tau) + G_{drc}(\tau) + G_{th}(\tau) \tag{4}$$

Indices elst, drc, and th refer to the electrostatic, dispersion-repulsion-cavity, and thermal free energy terms, respectively. All terms in eq 4 depend on the O=N−O−O torsion angle, τ.

If $ONOO^-$ has local free-energy-minimum structures at different τ angles, then the solute forms a mixture of conformers. To characterize $ONOO^-$ in aqueous solution, the composition of the mixture is to be determined. The equilibrium concentrations depend on relative standard free energy terms, thus relative instead of absolute free energies will be the focus of our study. For the reference structure, the cis $ONOO^-$ has been selected with $\tau = 0$. Accordingly, the

$$\Delta G_{stot}(\tau) = \Delta G_{elst}(\tau) + \Delta G_{drc}(\tau) + \Delta G_{th}(\tau) \tag{5}$$

terms will be investigated in the PCM calculations. In the (ab initio or DFT)/Monte Carlo calculations, the in-solution total relative free energy of the conformers are

$$\Delta G_{stot}(\tau) = (\Delta E(\tau, \text{int}) + \Delta G_{th}(\tau)) + \Delta G(\tau, \text{solv}) \tag{6}$$

where the internal free-energy term, $\Delta G(\tau, \text{int}) = \Delta E(\tau, \text{int}) + \Delta G_{th}(\tau)$ has been calculated quantum chemically, and $\Delta G(\tau, \text{solv})$ has been calculated upon the free energy perturbation method.

The solute's electrostatic free energy in a continuum solvent can be expressed as[9,10]

$$G_{elst} = E_s^\circ + 0.5E_{susv} = E_s - 0.5E_{susv} \tag{7}$$

with energy terms defined in eq 3. The difference of the solute energy in solution and in the gas phase is

$$E_s - E_g = E_s^\circ + E_{susv} - E_g = (E_s^\circ - E_{gs}) + (E_{gs} - E_g) + E_{susv} \equiv E_{supol} + E_{geom} + E_{susv} \tag{8}$$

In eq 8, a new partitioning of the $E_s - E_g$ energy has been suggested. The solute polarization energy is defined as $E_{supol} = E_s^\circ - E_{gs}$ and a geometry distortion term as $E_{geom} = E_{gs} - E_g$. E_{supol} is similar to the term E_{dist} of Orozco et al.,[11] while E_{geom} is new due to allowing different geometries in the gas phase and in solution. (Not indicated, but all terms in eqs 7 and 8 depend on the τ torsion angle.)

Relative thermal corrections, $\Delta G_{th}(\tau)$ and $\Delta\Delta G_{th}(\tau)$ are defined as follows:

$$\Delta G_{th}(\tau) = G_{th}(\tau) - G_{th}(0) \tag{9a}$$

$$\Delta\Delta G_{th}(\tau) = \Delta G_{ths}(\tau) - \Delta G_{thg}(\tau) \tag{9b}$$

$\Delta G_{th}(\tau)$ in eq 9a can be applied both for the solute or for the gas-phase molecule. Thus, subscripts "ths" and "thg" in eq 9b are used to refer to the in-solution and the gas-phase terms, respectively.

TABLE 1: Geometric Parameters Optimized at the B3LYP/6-311+G* Level in Aqueous Solution[a]

ONOO(τ)	O=N	N−O	O−O	ONO	NOO
0	1.208 (−5)	1.364 (−2)	1.393 (5)	115.9 (5)	117.6 (8)
30	1.207 (−7)	1.367 (1)	1.410 (5)	116.0 (−7)	117.8 (−10)
60	1.196 (−12)	1.394 (14)	1.456 (5)	115.3 (−10)	115.5 (−2)
77.3	1.179 (−13)	1.451 (36)	1.487 (−16)	113.0 (−10)	101.6 (0)
90	1.182 (−11)	1.483 (15)	1.469 (−3)	112.1 (−6)	92.0 (15)
120	1.196 (−12)	1.416 (14)	1.447 (7)	111.4 (−1)	103.4 (−21)
150	1.212 (−11)	1.362 (8)	1.420 (5)	111.0 (−1)	111.5 (−12)
180	1.217 (−11)	1.345 (8)	1.412 (4)	111.0 (−2)	113.1 (−10)

[a] Bond lengths in Å, bond angles and ONOO torsion angles in deg. Values in parentheses are the deviations from the corresponding geometric parameter optimized in the gas phase.[4] Deviations in units of the last decimals of the data in the table.

TABLE 2: Calculated Frequencies at the B3LYP/6-311+G* Level in Aqueous Solution[a]

ONOO(τ)	NOO_{bend}	$ONOO_{tors}$	$O-O_{str}$	ONO_{bend}	$N-O_{str}$	$O=N_{str}$
0	344 (12)	494 (−2)	830 (−3)	966 (−3)	728 (8)	1544 (29)
30	308 (4)	420 (−3)	814 (−5)	933 (−3)	711 (−2)	1541 (35)
60	294 (4)	303i (35i)	766 (−16)	837 (−12)	605 (−31)	1581 (65)
77.3	266 (−7)	617i (1i)	741 (−15)	814 (−10)	505 (−74)	1682 (76)
90	250 (−3)	134 (−66)[b]	715 (−18)	886 (−9)	481 (−24)	1660 (67)
120	402 (−4)	180i (26i)	702 (−10)	944 (−18)	573 (−13)	1601 (67)
150	415 (−6)	172 (−30)	615 (−2)	1001 (−9)	786 (−20)	1552 (57)
180	416 (−5)	232 (−23)	627 (1)	1018 (−6)	834 (−18)	1543 (56)

[a] Frequencies in cm^{-1}. Values in parentheses are the deviations from the corresponding frequencies obtained in the gas phase.[4] [b] The real, instead of an imaginary, frequency is considered as a numerical sensitivity of the frequency determination procedure when calculating near zero frequencies with default parameters of Gaussian. The real value at $\tau = 90°$ suggests a high-lying local minimum between $\tau = 77.3°$ and 120°. However, a geometry optimization started at $\tau = 95°$ led to a rapid energy decrease, while τ increased through 120° to 180°.

The $G_{th}(\tau)$ term for the gas-phase molecule was calculated in the classical limit of the rigid rotator, harmonic oscillator approximation[12] as $G_{thg}(\tau, \text{ideal gas}) = \text{ZPE} + (H_v(T) - \text{ZPE}) - TS(T) + 4RT$. ZPE, $H_v(T)$, and $S(T)$ are the zero point energy, the vibrational enthalpy at T, and the entropy at T, respectively. S includes a contribution of $R\ln 2$ for all nonplanar conformers, where a mixing of mirror image conformers is possible. The expression for G_{th} in solution is

$$G_{ths} = \text{ZPE} + (H_v(T) - \text{ZPE}) - TS(T) + 4RT + \Delta_{sg} \quad (9c)$$

The first three terms are to be calculated in the rigid rotator, harmonic oscillator approximation at the molecular geometry optimized in solution. Δ_{sg} stands for all corrections for the translational and rotational enthalpy and entropy, which were calculated in the-ideal gas approximations not directly applicable in a cavity-in-continuum model. Most likely, however, Δ_{sg} is nearly constant for the different conformers, thus does not appear in the ΔG_{ths} term.

Gas-phase calculations were performed at the ab initio MP2/6-311+G* level[13] and by means of the B3LYP functional in DFT[14] using the 6-311+G* basis set. The geometry of the $O_1=N_2-O_3-O_4^-$ anion was optimized at fixed torsion angles of $\tau = 0$, 30, 60, 90, 120, 150, and 180°. The torsion angle was set to $\tau = 0°$ and 180° for the planar cis and trans $ONOO^-$, respectively (Scheme 1). Calculations with torsion angles $\tau = 80.5°$ and 77.3°, corresponding to gas-phase transition states (TS) at the MP2 and B3LYP levels,[4] have been also carried out. Frequency analyses were performed for all gas-phase optimized geometries at the corresponding level. For direct comparability, the torsion reaction coordinate was considered as having thermal contribution to the vibrational free energy unless the frequency was imaginary. All calculations were performed with the Gaussian 98 package[15] implemented to the T90 computer at the Ohio Supercomputer Center.

Continuum-solvent calculations were performed by using the self-consistent isodensity polarizable continuum model,[8a] SCI−PCM, at the B3LYP/6-311+G* level. The isodensity contour parameter was set to 0.001 au, and 512 grid points were considered for the surface charges. The solvent dielectric constant was set to 78.3, corresponding to the dielectric constant of water at $T \approx 298$.[8b] The solute geometry was optimized at torsion angles mentioned above for the gas-phase calculations. In-solution geometric parameters and normal frequencies are provided in Tables 1 and 2. Relative energies are collected in Table 3. Subscripts g, s, and gs refer to optimized gas-phase, in-solution energies, and gas-phase energies at molecular geometries optimized in solution, respectively, as defined in eqs 3a−c.

TABLE 3: Conformational Energies Relative to ONOO ($\tau = 0$), Obtained with the 6-311+G* Basis Set[a]

ONOO(τ)	$B3LYP_g$ ΔE_g	$B3LYP_s$ ΔE_s^o	$B3LYP_{gs}$ ΔE_{gs}	$MP2_g$ ΔE_g
30	5.98	6.07	5.97	6.99
60	20.10	20.68	20.19	21.58
77.3	26.96	27.89	27.12	
80.5				26.22
90	24.23	24.77	24.29	25.46
120	17.18	17.71	17.25	19.38
150	7.42	7.58	7.46	8.39
180	3.29	3.30	3.32	3.49

[a] Relative energies in kcal/mol. For definitions of the energy terms, see eqs 3a−c. Subscripts g and s refer to optimization in the gas phase and in aqueous solution, respectively. Subscript gs means a gas-phase single-point calculation at the geometry optimized with the continuum-dielectric solvent model. Absolute energies in a.u. for ONOO ($\tau = 0$), in the order of columns: (B3LYP) −280.371270, −280.368699, −280.371119; (MP2) −279.699999.

Thermal corrections were calculated at $T = 298.15$ for the in-solution optimized structures. These values are in conformity with the dielectric constant of 78.3 accepted here. For the evaluation of the cis−trans free energy separation for the $ONOO^-$ anion in a biological environment, thermal corrections based on the gas-phase $MP2_g$ results were also calculated at $T = 310$ corresponding to the temperature in humans (Table 4).

The relative conformational solvent effect, $\Delta G_{SE}(\tau)$, has been defined on the basis of terms in eqs 3−9 as follows (all terms

TABLE 4: Free-energy Correction Terms Relative to ONOO ($\tau = 0$)[a]

	$T = 298.15$		$T = 310$
	B3LYP/gas	B3LYP/sol	MP2/gas
transition state[b]			
ZPE	−1.20	−1.29	−1.28
$H_\nu(T)$ − ZPE	−0.02	0.03	0.00
$TS(T)$[c]	0.45	0.53	0.51
$G_{th} = H_\nu(T) - TS(T)$	−1.66	−1.79	−1.79
ONOO(τ) = 90			
ZPE	−0.99	−1.12	−1.38
$H_\nu(T)$ − ZPE	0.38	0.47	0.05
$TS(T)$[c]	1.14	1.42	0.62
$G_{th} = H_\nu(T) - TS(T)$	−1.75	−2.06	−1.95
ONOO(τ) = 180			
ZPE	−0.28	−0.34	−0.19
$H_\nu(T)$ − ZPE	0.12	0.15	0.15
$TS(T)$	0.05	0.14	0.10
$G_{th} = H_\nu(T) - TS(T)$	−0.21	−0.32	−0.14

[a] Energy terms in kcal/mol. Since all values in the table are relative values with reference to the corresponding term with ONOO ($\tau = 0$), the G_{th} terms correspond to $\Delta G_{th}(\tau) = G_{th}(\tau) - G_{th}(0)$ in eq 9a. [b] Transition state indicates ONOO torsion angle of $\tau = 77.3$ and 80.5 for the B3LYP and MP2 calculations, respectively. For further explanation, see also the text. [c] These entropy terms contain a contribution of RT ln 2 due to the mixing of mirror-image antipodes. No such a correction is necessary for the planar trans form.

depend on τ, subscripts "stot" and "g" refer to the $ONOO^-$ free energy in solution and in the gas phase, respectively):

$$\Delta G_{SE} \equiv \Delta G_{stot} - \Delta G_g = (\Delta E_{geom} + \Delta\Delta G_{th} + \Delta E_{supol}) + (0.5\Delta E_{susv} + \Delta G_{drc})$$

$$\equiv \Delta G(\text{int}) + \Delta G(\text{solv}) \quad (10a)$$

The intramolecular free energy change, $\Delta G(\text{int}) = \Delta E_{geom} + \Delta\Delta G_{th} + \Delta E_{supol}$, accounts for changes in the solute geometry and thermal corrections and takes into consideration the solute polarization energy. $\Delta G(\text{solv}) = 0.5\Delta E_{susv} + \Delta G_{drc}$ stands for the relative solvation free energy. The present partitioning of ΔG_{SE} makes possible the direct comparison of the $\Delta G(\text{solv})$ term with that from Monte Carlo simulations (see below).

Relative solute−solvent interaction energies (ΔE_{susv}) are summarized in Table 6. ΔE_{supol}, ΔE_{geom}, and $\Delta\Delta G_{th}$ were calculated on the basis of eqs 8 and 9, using data from Tables 3 and 4. Free energy contribution terms from continuum solvent calculations (Table 7) include ΔG_{elst}, eq 7, and the dispersion-repulsion-cavity term, ΔG_{drc}. (It is to be mentioned that the Gaussian 98 output for the SCI−PCM method provides G_{elst} directly as the SCF energy. After having obtained the optimized geometry, a single-point calculation was performed to calculate the relevant solute−solvent interaction energy (0.5 E_{susv} appears in the output), the final SASA term (see below), and the molecular volume. Using eq 7, $E_s°$ was calculated.) The ΔG_{drc} term is the sum of the dispersion-repulsion, ΔG_{dr}, and the cavity formation, ΔG_c, relative free energy contributions. ΔG_{dr} was calculated by using the formula of Floris and Tomasi,[16] which establishes correlation between the dispersion-repulsion free energy and the molecular surface. The molecular surface was considered here as the solvent-accessible surface area (SASA). ΔG_c was calculated based on the Pierotti formula[17] as provided by Claverie at al.[18] Courses of the changes in the E_{supol}, $G(\text{solv})$, and ($G(\text{solv}) + E_{supol}$) terms are shown in Figure 1, dipole moments are compared in Figure 2.

Monte Carlo simulations[19] for the $ONOO^-$ anion in aqueous solution were performed by using the BOSS 3.6 software[20] on a Silicon Graphics Indigo 2 workstation. Calculations were performed in the NpT (isobaric−isothermal ensembles) at $T =$ 310 and $p = 1$ atm. The 24 × 24 × 24 Å^3 periodic box contained one solute and 508 TIP4P water molecules.[21] Preferential sampling proportional to $1/(R^2 + c)$ was applied, with a value of 120 for the constant c. R is the distance between the N atom of the solute and the oxygen atom of a water molecule to be displaced in generating a new configuration. The solvent−solvent cutoff radius was set to 8.5 Å. With a solute−solvent cutoff radius, SCUT, of 12 Å, all solvent molecules were seen by the solute within spheres of $R = 12$ Å around any solute atoms (BOSS option ICUT = 2). 3500 and 5000 K configurations were generated in the equilibrium and averaging phases, respectively. Solute move was attempted every 50 steps, volume changes with a maximum of 250 Å^3 were allowed in every 1000 steps.

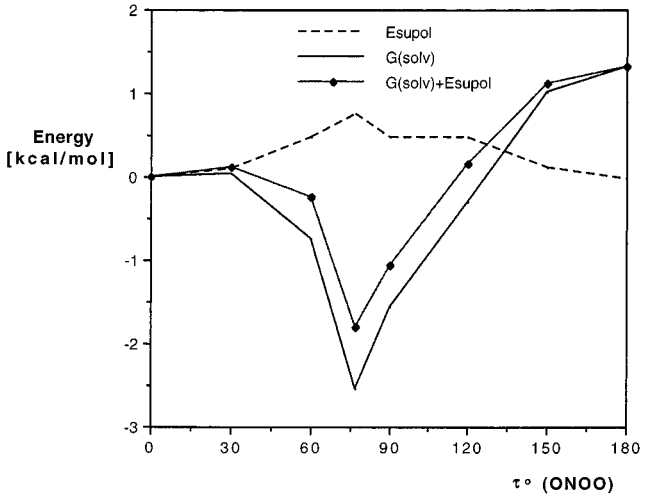

Figure 1. Change of the solute polarization energy, $E_{supol} = E_s° - E_{gs}$ (dashed line) and the solvation free energy, $G(\text{solv}) = 0.5E_{susv} + G_{drc}$ (solid line) calculated with the SCI−PCM method. The sum of the two terms is indicated with marked solid line.

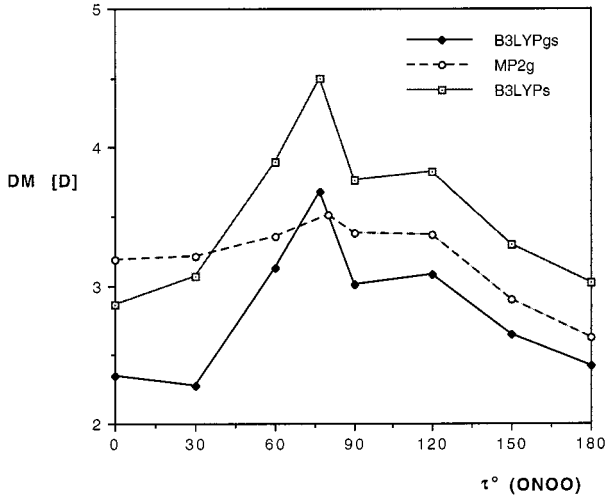

Figure 2. Dipole moments calculated from atomic charges fitted to the 6-311+G* molecular electrostatic potentials, and using the standard orientation in the coordinate system by Gaussian 98. Deviations from the exact values are up to 0.2 D. Indices g and s refer to the gas phase and solution, respectively. For models with single-letter subscripts, the charges were fit to electrostatic potentials calculated in the phase of the geometry optimization. Charges for the model with gs subscripts were fit to the gas-phase ELPO calculated at the in-solution optimized geometry.

TABLE 5: Electrostatic Potential Fitted Atomic Charges[a]

	ELPO				CM2			
ONOO(τ)	O═	N	O	O^-	O═	N	O	O^-
				Case A				
0	−0.288	−0.005	−0.087	−0.620	−0.287	−0.067	0.028	−0.674
80.5	−0.232	0.064	−0.245	−0.587	−0.184	0.048	−0.187	−0.677
90	−0.242	0.071	−0.233	−0.596	−0.199	0.066	−0.190	−0.677
180	−0.471	0.187	0.000	−0.716	−0.379	0.029	0.027	−0.677
				Case B				
0	−0.259	−0.079	−0.060	−0.602	−0.250	−0.049	−0.024	−0.677
77.3	−0.130	0.025	−0.225	−0.670				
90	−0.162	0.009	−0.218	−0.629	−0.175	0.054	−0.196	−0.683
180	−0.378	0.057	0.042	−0.721	−0.341	0.029	−0.010	−0.678
				Case C				
0	−0.251	−0.138	−0.052	−0.559				
77.3	−0.158	−0.027	−0.209	−0.606				
90	−0.190	−0.037	−0.208	−0.565				
180	−0.421	0.052	0.065	−0.696				

[a] ELPO charges fitted to the molecular electrostatic potential by the CHELPG procedure. CM2 charges were obtained from AMSOL 6.6 using the PM3 Hamiltonian. Case A: HF/6-311+G* gas-phase ELPO and gas-phase CM2 charges, MP2/6-311+G* gas-phase geometry. Case B: B3LYP/6-311+G* in-solution ELPO and gas-phase CM2 charges, B3LYP/6-311+G* in-solution geometry. Case C: B3LYP/6-311+G* gas-phase ELPO charges, B3LYP/6-311+G* in-solution geometry.

TABLE 6: B3LYP/6-311+G* Relative Electrostatic, Geometric and Frequency Dependent Energy Terms Contributing to the Solvent Effect in the Continuum Dielectric Approach[a]

ONOO(τ)	$0.5\Delta E_{susv}$	ΔE_{supol}	ΔE_{geom}	$\Delta\Delta G_{th}(\tau)$
30	0.00	0.10	−0.01	−0.02
60	−0.77	0.49	0.08	−0.05
77.3	−2.57	0.76	0.16	−0.13
90	−1.56	0.49	0.05	−0.31
120	−0.33	0.47	0.06	−0.04
150	0.99	0.11	0.04	−0.14
180	1.30	−0.02	0.02	−0.11

[a] Energies in kcal/mol. $\Delta\Delta G_{th}(\tau) = \Delta G_{ths}(\tau) - \Delta G_{thg}(\tau)$, $G_{ths}(0) - G_{thg}(0) = 0.06$ kcal/mol. Reference values for ONOO ($\tau = 0$) in a.u: $0.5E_{susv} = -0.088313$, $E_{supol} = 0.002420$, $E_{geom} = 0.000151$.

TABLE 7: B3LYP/6-311+G* Free Energy Contribution Terms with the Continuum Solvent Model and Total Free Energies Relative to the ONOO ($\tau = 0$) Form in Aqueous Solution[a]

ONOO(τ)	ΔG_{elst}	ΔG_{drc}	ΔG_{ths}	ΔG_{stot}	ΔG(solv)	ΔG_g
30	6.07	0.03	−0.74	5.36	0.03	
60	19.91	0.03	−1.63	18.31	−0.74	
77.3	25.32	0.02	−1.79	23.55	−2.55	25.30
90	23.21	0.01	−2.06	21.16	−1.55	
120	17.39	0.03	−1.31	16.11	−0.30	
150	8.57	0.02	−1.08	7.51	1.01	
180	4.60	0.03	−0.32	4.31	1.33	3.08

[a] Energies in kcal/mol. $\Delta G_{stot} = \Delta G_{elst} + \Delta G_{drc} + \Delta G_{ths}$, $T = 298.15$. $\Delta G(\text{solv}) = 0.5\Delta E_{susv} + \Delta G_{drc}$, ΔG_g is the relative free energy in the gas phase. Values were calculated using those in Tables 3 and 6.

Intermolecular interactions were calculated with the 12−6−1 OPLS potential function.[22] Steric parameters were taken from the program's library. ELPO atomic charges (Table 5) were derived upon fitting charges to the molecular electrostatic potential[23] of the peroxynitrite anion by using the CHELPG procedure.[24] Molecular electrostatic potentials were calculated here by using the 6-311+G* wave functions in contrast to the HF/6-31G* electrostatic potential proposed by Carlson et al.[23a] For a comparison of atomic charge sets obtained with different basis sets, fitted charges have been derived here using both the HF/6-31G* and HF/6-311+G* molecular electrostatic potentials at different τ torsion angles. Differences did not exceed 0.05 charge units. Potential of mean force calculations for the *N*-trimethylaniline−acetate ion-pair showed a minor difference when the acetate atomic charges were derived from the HF/6-31G* and HF/6-31+G* electrostatic potentials.[25] Thus, inclusion of diffuse functions changes the atomic charges but the effect is not remarkable, at least on the PMF of an ion-pair. Depending on the accepted geometry, three different potential-fitted charge sets were derived for the $ONOO^-$ (Table 5).

The other group of charge sets includes the CM2 charges.[26] CM2 charges can be derived with the AMSOL 6.6 modeling software[27] both with fixed geometry and after geometry optimization, using the semiempirical AM1[28] or PM3[29] Hamiltonian. Charge sets in Table 5 were obtained at the indicated geometries and with the PM3 Hamiltonian for the gas-phase molecules. CM2/PM3 and CHELPG charges are mostly in qualitative agreement. In contrast, the CM2/AM1 charge is positive for the oxygen atom in the O═N bond. This is in qualitative disagreement with the results of Tsai et al.,[6] who pointed out that the O═ site is a strong hydrogen bond acceptor site in $ONOO^-$ hydrates.

Relative solvation free energies were calculated using the free-energy perturbation (FEP) method[30] as it was implemented in Monte Carlo simulations.[31] Geometric and OPLS potential parameters for the perturbed systems were calculated as a linear function of the perturbation step parameter, λ.[31] Using double-wide sampling, the perturbation pathway was the torsion of the molecule from the cis to the trans form in increments of $\Delta\tau \leq 7.5°$ for the ONOO torsion angle.

Long-range electrostatic effects were calculated in two ways. Interaction free energy with the solvent out of the explicitly considered solvent volume, thus beyond the overlapping spheres with R = SCUT = 12 Å around each solute atom, was calculated upon the charging work to develop the charge distribution in a dielectric continuum with dielectric constant ϵ.[32] The ϵ value was taken of 53, as calculated for the TIP4P water.[33] Differences of long-range electrostatic contributions were a few hundredths of a kcal/mol for different conformers. In another approach, the solute was characterized by its dipole moment, although its calculated value is not translationally invariant. The $ONOO^-$ dipole moments calculated by the Gaussian 98 software are in the range of 2.2−4.5 D. In the coordinate system by the BOSS software throughout MC simulations, the dipole moment calculated from the CHELPG atomic charges fell in the 5.7−7.7 D range. Using the Onsager

TABLE 8: Free Energy Contribution Terms from Monte Carlo Simulations and Total Free Energies Relative to the ONOO ($\tau = 0$) Form in Aqueous Solution[a]

	ΔG(solv)				
ONOO(τ)	B3LYP$_s$	B3LYP$_{gs}$	MP2$_g$ELPO	MP2$_g$CM2	ΔG_{thg}[b]
30	−0.26 ± 0.07	0.12 ± 0.07	0.42 ± 0.07	−0.12 ± 0.07	−0.74
60	−3.35 ± 0.11	−1.28 ± 0.10	0.49 ± 0.11	−2.01 ± 0.13	−1.52
TS	−7.97 ± 0.12	−4.76 ± 0.12	−0.53 ± 0.12	−3.96 ± 0.15	−1.79
90	−4.33 ± 0.13	−2.32 ± 0.13	−0.34 ± 0.13	−3.37 ± 0.15	−1.95
120	−2.55 ± 0.15	−1.02 ± 0.17	0.74 ± 0.17	−0.16 ± 0.20	−1.28
150	−0.47 ± 0.18	−0.33 ± 0.19	0.93 ± 0.20	3.91 ± 0.22	−0.87
180	−0.46 ± 0.19	−1.23 ± 0.22	−0.07 ± 0.23	4.96 ± 0.24	−0.14

	$\Delta G_{stot}[c] = \Delta E + \Delta G_{th} + \Delta G$(solv)				
ONOO(τ)	B3LYP$_s$	B3LYP$_{gs}$	MP2$_g$ELPO	MP2$_g$CM2	ΔG_g[d]
30	5.07	5.35	6.67	6.13	
60	15.70	17.28	20.55	18.05	
TS	18.13	20.57	23.90	20.47	24.43
90	18.38	19.91	23.17	20.14	
120	13.85	14.92	18.84	17.94	
150	6.03	6.05	8.45	11.43	
180	2.52	1.77	3.28	8.31	3.35

[a] Energies in kcal/mol. [b] ΔG_{thg} for the MP2/6-311+G* optimized structure in the gas phase at $T = 310$. [c] For the ΔE term, $\Delta E_s°$ was accepted for B3LYP$_s$, ΔE_{gs} for B3LYP$_{gs}$, and ΔE(int) for the MP2$_g$ calculations. For the corresponding ΔE terms, see Table 3. ΔG_{th} for the B3LYP calculations was taken from Table 7, ΔG_{thg} in the present table was used with the MP2 series. ΔG_{stot} values have the same standard deviations as the corresponding ΔG(solv) terms. [d] Relative MP2$_g$ free energies in the gas phase at $T = 310$.

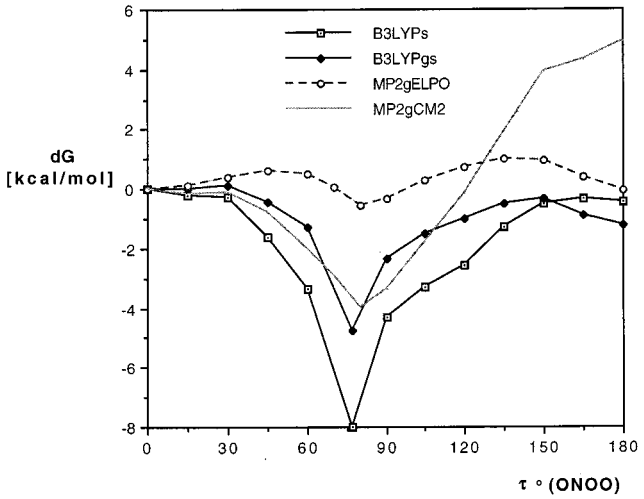

Figure 3. Relative solvation free energies calculated upon Monte Carlo simulations. For subscripts, see the footnote for Figure 2. Extensions ELPO and CM2 refer to charge sets A in Table 5.

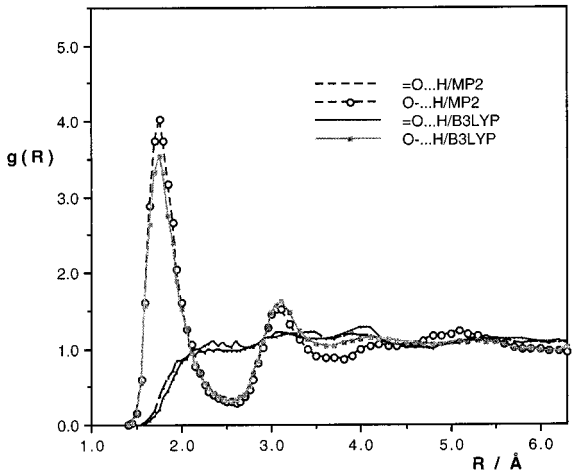

Figure 4. Radial distribution functions for the cis ONOO$^-$ conformer: $=O_1\cdots H_w$ (unmarked line) and $O_4{}^-\cdots H_w$ (marked line). All curves with ELPO charge parameters (sets A/ELPO and B/ELPO in Table 5), with MP2$_g$ and B3LYP$_s$ geometries. For the subscript code, see the footnote for Figure 2.

correction[34] for a dipole in the cavity of $R \approx 13$ Å, corresponding to the union volume of overlapping spheres with 12 Å individual radii, the calculated relative long-range electrostatic interaction energy was no more than 0.1 kcal/mol even with dipole moment changes as large as 5.5 to 8.1 D with the CM2 charges.

MC calculations were performed with rigid molecular geometries optimized in the gas phase at the MP2/6-311+G* level and with solutes optimized in solution at the B3LYP/6-311+G* level. Two series of calculations with ELPO and CM2 charges (case A, Table 5) have been performed with the MP2 solute. The ELPO charges were utilized in case B (B3LYP$_s$), and set C was used when the gas-phase charges were derived at the B3LYP in-solution geometry (B3LYP$_{gs}$). Relative solvation free energies, including long-range electrostatic corrections are summarized in Table 8 and shown in Figure 3. Solution structure has been characterized on the basis of MC simulations. Radial distribution and pair-energy distribution functions are provided in Figures 4−8.

Results and Discussion

Geometries and Vibrational Frequencies. The center of interest in this paper is the comparison of the results obtained with a continuum-dielectric solvent method with those from an (ab initio or DFT)/Monte Carlo approximation. Peroxynitrite anion has been selected here for two reasons. It is a biologically important molecule and conformational analysis for that in aqueous solution may draw interest by itself. Furthermore, the small number of atoms in this molecule allows a detailed analysis of factors influencing solvent effects, and to find correspondence of free-energy contribution terms in the two applied approaches.

In-solution optimized geometric parameters are summarized in Table 1. Values in parentheses show the deviation of the in-solution geometry from its gas-phase counterpart. All internal coordinates but the O=N−O angle undergo remarkable changes with, in general, extreme values in the range of $\tau = 77°-90°$. Large changes upon torsion have been found for the N−O

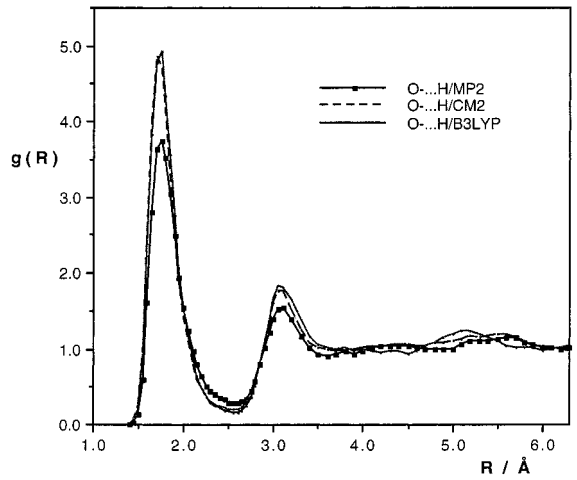

Figure 5. $O_4^-\cdots H_w$ radial distribution functions for the $ONOO^-$ anion at the gas-phase transition state torsion angles. MP2 and CM2 curves with ELPO and CM2 charges (sets A), respectively, for the solute with $MP2_g$ gas-phase optimized geometry. B3LYP refers to a solute with ELPO charges and in-solution optimized geometry ($B3LYP_s$, set B/ELPO in Table 5).

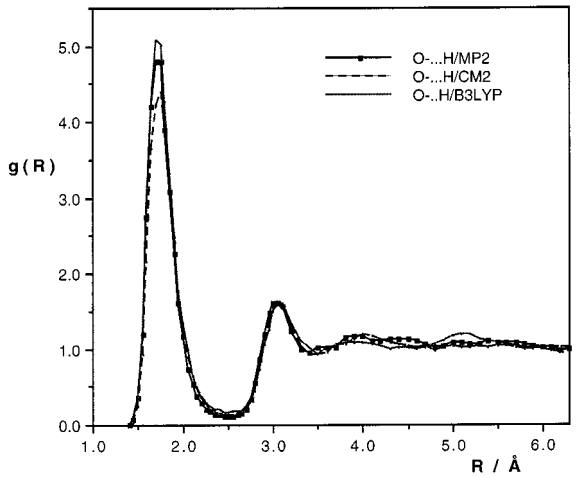

Figure 6. $O_4^-\cdots H_w$ radial distribution functions for the trans $ONOO^-$ anion. For the letter code, see the footnote in Figure 5.

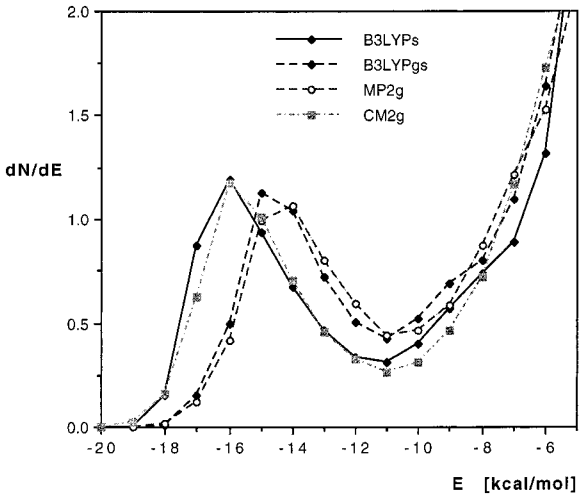

Figure 7. Pair-energy distribution functions for the $ONOO^-$ anion at the gas-phase transition state torsion angles. For the subscript code, see the footnote in Figure 2. $CM2_g$ refers to the $MP2_g$ geometry with CM2 charges (set A in Table 5). All other curves were calculated using ELPO charge sets.

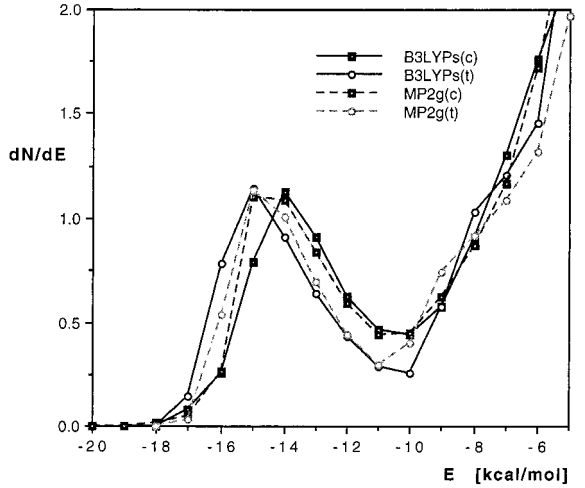

Figure 8. Pair-energy distribution functions for the cis (c) and trans (t) $ONOO^-$ anion calculated with the ELPO charges (sets A/ELPO and B/ELPO in Table 5). For the subscript code, see the footnote in Figure 2.

(central bond) distance and for the $O-O^-$ distance, both in the gas-phase and in solution. Whereas the ONO angle decreases moderately throughout the cis to trans rotation, the NOO angle takes a minimum value at $\tau = 90°$ with a deviation of 21°−26° from the equilibrium values in the planar conformations.

Frequency shifts upon solvation are small, except those for the O═N and N−O stretching vibrations. The two largest shifts were calculated here at 76 and -74 cm^{-1}, following a relatively small shortening of the O═N bond by 0.013 Å, and the large, 0.036 Å increase of the N−O distance, respectively, at $\tau =$ 77.3°. The largest increase in bond angles was calculated at 1.5° for the NOO angle, which caused a frequency shift of only -3 cm^{-1}. These calculated shifts, however, must be taken with caution, because only the cis and the trans conformers correspond to local energy minima both in the gas phase and in solution.

Tsai et al.[4] calculated gas-phase optimal geometries and vibrational frequencies at several levels including B3LYP and CCSD, and using the 6-311+G* basis set. The O═N distance and the bond angles differed by less than 0.01 Å and by 1−2°, respectively, at the two levels. The O═N stretching and the bending frequencies differed by up to 70 cm^{-1}, but calculated frequencies in the cis conformation were still close to the experimental values. Whereas all frequencies but the ONOO torsion are close to the experimental values at the CCSD level in the cis conformation, the B3LYP N−O stretching frequencies are smaller than the CCSD values by 245−285 cm^{-1} in the planar forms. (Geometry, but not frequencies, was provided for the CCSD transition state structure.) The B3LYP red-shift is due to the consistently longer by 0.023−0.036 Å N−O distances at the B3LYP as compared to the CCSD level. In contrast, differences of the N−O stretching frequencies between the cis and trans conformers are similar, 132 and 92 cm^{-1} at the B3LYP and CCSD levels, respectively. The difference of the cis−trans N−O stretching frequencies by B3LYP in solution is 106 cm^{-1}, being consistent with the gas-phase value.

Energies and Thermal Corrections. Relative energies are summarized in Table 3. All calculations show a large barrier to rotation when transforming the molecule from the cis to the trans form. The barrier is 26−28 kcal/mol at the B3LYP and MP2 levels, both in the gas phase and in solution. The cis form is lower in energy than the trans by about 3.3 kcal/mol, both in the gas phase and in solution, at the B3LYP/6-311+G* level. Geometry changes have practically no effect on the cis−trans

energy separation of the $ONOO^-$ anion. MP2 calculations, performed only in the gas phase, predict the stabilization of the cis conformer by 3.5 kcal/mol. (Calculations at the HF/6-311+G* level predicted a barrier of about 15 kcal/mol, and found the trans conformer to be of lower energy by about 2 kcal/mol than the cis form, both in the gas phase and in solution. Since these results are in contrast to all higher level calculations both in the present study and in ref 4, and are in contrast to the explanation of the experimental Raman spectrum,[5] HF calculations have not been further considered.)

Gas-phase calculations of Tsai et al.[4] at the CCSD(T)/6-311+G*//CCSD/6-311+G* level found relative energies of 23.8 and 2.8 kcal/mol for the TS ($\tau = 80.3°$) and the trans forms, respectively. Their results indicate the importance of high-level calculations for the $ONOO^-$ anion, since the relative energies for the conformers are not converged even at the CCSD/6-311+G* level. The CCSD and the single-point CCSD(T) relative energies for the TS and the trans forms differ by 2.4 and 1.2 kcal/mol, respectively. From the point of view of the present study it is promising that the B3LYP relative trans energy, 3.3 kcal/mol, differs by only 0.5 kcal/mol from the high-level CCSD(T) value.

Thermal contributions to the free energy are compared in Table 4. In-solution terms were calculated at $T = 298.15$, using a dielectric constant of $\epsilon = 78.3$. (B3LYP/SCI−PCM calculations of Tsai et al.[4] were performed with $\epsilon = 80.0$) The largest contribution to the relative $G_{th} = G(T)$ stems from the relative zero point energy, ZPE. This latter value is around −1 kcal/mol for the TS structure and at $\tau = 90°$, but is only about −0.2 to −0.3 kcal/mol for the trans form. For this conformer, $G(T)$ is almost equal to ZPE as a consequence of the cancellation of the ($H_\nu(T)$ − ZPE), vibrational thermal enthalpy, and the $TS(T)$ terms. The near cancellation mostly applies for other conformations as well, if the RT ln 2 term (0.41−0.43 kcal/mol), included in $TS(T)$ due to the mixing of the mirror-image antipodes, is subtracted from $TS(T)$.

The B3LYP G_{th} values in Table 4 differ by no more than 0.31 kcal/mol if the corresponding gas-phase and in-solution values are compared. Furthermore, the B3LYP and MP2 relative gas-phase values at $T = 298.15$ and $T = 310$, respectively, are similar. These results call the attention that relative conformational G_{th} values in solution can be usefully approximated by values obtained for gas-phase structures.

Most of the biologically important molecules are biopolymers or at least large molecules. On the other hand, there are smaller systems with equally important biological effects. For technical reasons, large systems can be studied today only at molecular mechanics level. Quantum mechanical/statistical mechanical treatment is feasible, however, for systems with 10−20 CNO atoms and connecting hydrogens. Several theoretical studies considering solvent effects have been performed recently for such important molecules as neurotransmitters (histamine,[35] dopamine,[36] GABA,[37] noradrenaline[38]), simple zwitterionic amino acids,[39] and for molecules providing important substructures in drugs and natural substances.[40] These molecules have several rotatable bonds, making the exploration of the potential energy surface very time consuming. Hundreds of geometry optimizations in solution and thermal correction calculations for the proper determination of the free energy (relative free energy) in solution require a theoretical method that can be used routinely at relatively low computational cost. Calculation of the thermal correction for gas-phase molecules could reduce the necessary computer time. Whereas in-solution optimization at the DFT level seems to be necessary in many cases for obtaining relevant geometry for further considerations (see next section), a combination of the DFT geometry optimization in a continuum solvent and determination of the ΔG_{th} term in the gas phase may be faster than a full in-solution determination of the conformational $\Delta E + \Delta G_{th}$ term at the DFT level, mainly with higher basis sets.

Relative Free Energies in Solution. For chemical equilibria, the equilibrium constant, K, is related to the change of the standard free energy, $\Delta G°$, as $-RT \ln K = \Delta G°$ Thus, if the composition of a mixture of conformers is to be determined, $\Delta G°$ rather than ΔE is the useful thermodynamic parameter. It will be pointed out in this section that whereas the ΔE and $\Delta G°$ values, due to the small relative thermal correction, differ only slightly for the cis and trans forms in the gas phase, the relative energy and free energy terms are remarkably different for these conformers in aqueous solution.

The relative conformational solvation free energy with the continuum dielectric solvent model was defined in eq 10a. ΔG(solv) does not contain the solute polarization and geometry distortion terms (ΔE_{supol} and ΔE_{geom}, respectively) and may be directly compared with the ΔG(solv) values from Monte Carlo simulations using the OPLS potential and a rigid solute geometry. Indeed, in the present MC application, the interaction energy of an *already* polarized solute and an *already* polarized solvent system is calculated, with no consideration to the free energy expense for polarizing the elements of the solution. This free energy will be considered upon the ΔG(int) term defined in eq 6 for the (ab initio or DFT)/MC model.

Terms appearing in eq 10a are summarized in Tables 6 and 7. The term $0.5\Delta E_{susv}$ shows a deep minimum of −2.57 kcal/mol at $\tau = 77.3°$. The course of the ΔE_{supol} curve is opposite, with a maximum of 0.76 kcal/mol at the (gas-phase) TS structure. ΔG(solv) is close to $0.5\Delta E_{susv}$ at any rotations because the calculated ΔG_{drc} term is almost negligible (Table 7). Although the individual G_{dr} terms amounted to as much as about −6.7 kcal/mol calculated upon the surface-dependent formula of Floris and Tomasi,[16] the relative ΔG_{dr} terms varied only between 0 and −0.14 kcal/mol. The absolute G_c terms[18] also have large values of about 8.9 kcal/mol, but the ΔG_c terms were calculated in the range of 0−0.17 kcal/mol. Due to the term cancellation, $\Delta G_{drc} = \Delta G_{dr} + \Delta G_c$ was calculated always as a small positive value of no more than 0.03 kcal/mol. Thus $\Delta G(\text{solv}) \cong 0.5\Delta E_{susv}$ has a minimum value of −2.55 kcal/mol.

Figure 1 shows the courses of the ΔE_{supol}, ΔG(solv), and $\Delta G(\text{solv}) + \Delta E_{supol}$ curves. Throughout the entire rotation range, ΔG(solv) is the dominant component. ΔE_{supol} is about 0 kcal/mol for the trans form, where both the ΔE_{geom} and the $\Delta\Delta G_{th}$ terms are small. As a consequence, the solvent effect for the trans form is practically reduced to $0.5\Delta E_{susv}$, which was calculated as a considerably positive value by the SCI−PCM method (Table 6).

In a reordered form of eq 10a:

$$\Delta G_{stot} = (\Delta E_{supol} + 0.5\Delta E_{susv} + \Delta G_{drc}) + (\Delta E_{geom} + \Delta\Delta G_{th}) + \Delta G_g \quad (10b)$$

the first term in eq 10b has strongly negative (−1.79 kcal/mol) and positive (1.31 kcal/mol) values for the TS and trans structures, respectively. Since the second term varies between 0.03 and −0.26 kcal/mol (Table 6), the solvation contribution to the total relative conformational free energy in solution is primarily determined by the first term. Accordingly, the free energy decreases and increases for the TS and trans conformers, respectively, as compared to their gas-phase values.

Relative solvation free energies calculated in Monte Carlo simulations are compared in Figure 3. All ΔG(solv) curves show a minimum around $\tau = 80°$ and, with the exception of the $MP2_g$-CM2 values, ΔG(solv) is within the -1.2 to -0.1 kcal/mol range for the trans form at $\tau = 180°$ (Table 8). The depth of the minimum at TS depends both on the solute geometry and the charge parameters. For the MP2 curves (sets A in Table 5) the gas-phase geometry was used. With the gas-phase ELPO charges, the minimum is shallow and the solvent effects are modest in the entire τ range. Use of CM2 charges led to considerable stabilization of the TS structure but large destabilization of the trans form by about 5 kcal/mol relative to the cis conformer.

Tsai et al.[6] found that the $ONOO^-\cdots H_2O$ binding energy is almost equal in the cis and trans forms when the water binds to the primary site at the O_4^- atom. Binding energy at the secondary site O_1= atom is reduced compared to that at the primary site by nearly the same amount for the two conformers. These results suggest no considerable difference in the hydration of the cis and trans forms, and validate a method that provides only a small value for the cis−trans relative solvation free energy. Simulations with the ELPO charges meet this expectation but not those with the CM2 parameterization. The slightly different dipole moments obtained with the two charge sets for the cis as well as for the trans conformers in Monte Carlo simulations suggest that the solvent "sees" the individual conformers similarly at some larger distance with either charge sets. The conformational changes, however, are followed by the ELPO rather than by the CM2 charges more sensitively: the O^- charge is almost constant in the CM2 set, and the O=N charges undergo smaller variation than the corresponding ELPO values. Taking all these findings together, simulations for $ONOO^-$ with ELPO charge sets are considered here more relevant than those with the CM2 charges.

In the other two simulations, in-solution optimized B3LYP geometries were studied. The applied charge sets strongly affect the courses of the solvation free-energy curves. For $B3LYP_s$ with the B/ELPO set, where the in-solution polarized charge distribution was approximated, ΔG(solv) is -8.0 kcal/mol for TS. The corresponding $B3LYP_{gs}$ value is -4.8 kcal/mol, in which case atomic charges were fit to the in-gas-phase molecular electrostatic potential (set C).

Combined analyses of Figures 2 and 3 conclude a complicated relationship between solute geometry and charges, on one hand, and ΔG(solv), on the other hand. $B3LYP_s$ and $B3LYP_{gs}$ dipole moments show an almost constant shift for all conformations. The peak in Figure 2 at the TS structure is in qualitative agreement with the strongly negative ΔG(solv) value at this geometry. However, the $B3LYP_s$ and $B3LYP_{gs}$ ΔG(solv) curves cross each other at $\tau = 150°$, in contrast to the dipole moment curves. The MP2 dipole moments have a slight maximum at $\tau = 80.5°$, whereas the ELPO and CM2 parameterization leads to very different stabilization of this conformer. For the trans form, ΔG(solv) is slightly negative (-0.1 kcal/mol) according to the $MP2_g$ELPO curve, while a large positive value was obtained with the CM2 parameterization.

The ΔG(solv) difference between $B3LYP_s$ and $B3LYP_{gs}$ emphasizes the importance of the reference electron distribution accepted when fitting the atomic charges. ΔG(solv) for TS is larger with charges fitted to an electrostatic potential created by a solute in solution than with charges derived from gas-phase electrostatic potentials. Charges fitted to the gas-phase HF/6-311+G* ELPO produce a much smoother course for the $MP2_g$ELPO curve compared to the $B3LYP_{gs}$ curve, for which atomic charges were obtained upon a fit to the gas-phase ELPO of the correlated DFT electron distribution. Since the solute geometry at a specific τ angle was identical for the $B3LYP_s$ and $B3LYP_{gs}$ calculations, and the corresponding MP2 geometry did not differ too much from that, it seems that charges rather than geometric changes have the larger effect on Monte Carlo relative solvation free energies.

In comparison, ΔG(solv) curves obtained from Monte Carlo simulations and calculated with the continuum model show similarities and remarkable differences, as well (Figures 1, 3). The most negative ΔG(solv) value has been found for the TS structure in all cases. The relative solvation free energy values from Monte Carlo simulations are in the range of -1.2 to -0.1 kcal/mol (± 0.2 kcal/mol) for the trans form (if the $MP2_g$CM2 value is disregarded). The corresponding value from SCI−PCM calculations is, however, $+1.3$ kcal/mol.

Total relative free energies calculated in the continuum solvent model approximation (Table 7) indicate that the cis form is more stable than the trans by 4.3 kcal/mol in aqueous solution. This is an increase in stability by 1.2 kcal/mol, as compared to the gas phase. The barrier has decreased by 1.8 kcal/mol in solution.

MC based ΔG_{stot} values show a large diversity (Table 8). In calculating this final thermodynamic quantity, qualitatively different ΔE terms were chosen. At the $B3LYP_s$ level, the solute's atomic charge parameters represented a polarized solute in solution. Thus $\Delta E = \Delta E_s°$ relative energies were considered (Table 3). The $B3LYP_{gs}$ solute was characterized by its gas-phase charge distribution, thus ΔE was set to ΔE_{gs}. MP2 solutes were accepted with their gas-phase geometry and charges, thus the MP2/6-311+G* relative internal energies, ΔE_g, were considered.

The B3LYP/MC results show the cis preference over the trans, but the cis stabilization is reduced to 1.8−2.5 kcal/mol as compared to the gas-phase value of 3.1 kcal/mol. The barrier has decreased by 4.7−7.2 kcal/mol relative to that in the gas phase. The $MP2_g$ELPO combination gives the closest results to the B3LYP continuum values regarding the cis stabilization and the barrier height. The cis form is more stable than the trans by 3.3 ± 0.2 kcal/mol, and the barrier is reduced by 0.5 ± 0.1 kcal/mol in solution. $MP2_g$CM2 predicts an extremely large (8.3 ± 0.2 kcal/mol) stabilization of the cis over the trans conformer in solution. With this parameterization the barrier is reduced by 4 kcal/mol to 20.5 kcal/mol, which is close to the values calculated with the B3LYP models (18.4−19.9 kcal/mol).

In the absence of experimental values for the cis−trans free-energy separation and for the free energy of the barrier, no choice for the useful method can be made. The peroxynitrite anion, which is stable in basic solution, must be the prevailing form at the physiological pH = 7.4, because acids, as weak as those with $pK_a = 6$, must be dissociated more than 90% at this pH. The experimental Raman spectrum was interpreted by Tsai et al.[5] so that the cis conformer is the existing form for the $ONOO^-$ anion in basic solution. The present results also find the cis form to be the most stable conformer in aqueous solution. It is important to emphasize, however, that the SCI−PCM and DFT/MC methods at the B3LYP/6-311+G* level provide different trends. In the continuum solvent approximation the cis conformer is further stabilized relative to the trans, when compared to the gas-phase value. On the basis of Monte Carlo results, the cis stabilization decreases in solution. Since the relative internal and solvation free-energy terms have opposite signs in this model, proper determination of both components is important in order to make a good theoretical estimate for

TABLE 9: Total Relative Free Energies and Calculated Equilibrium Constants[a]

	ΔG_g(TS)	$\Delta G_g(t)$	$K(t/c)$	ΔG_s(TS)	$\Delta G_s(t)$	$K(t/c)$
gas phase						
B3LYP	25.30	3.08	5.5×10^{-3} [b]			
MP2	24.43	3.35	4.3×10^{-3} [c]			
SCI−PCM						
B3LYP				23.55	4.31	6.9×10^{-4} [b]
Monte Carlo						
$B3LYP_{gs}$				20.57 ± 0.12	1.77 ± 0.22	5.7×10^{-2} [c,d]
$B3LYP_s$				18.13 ± 0.12	2.52 ± 0.19	1.7×10^{-2} [c,d]
$MP2_gELPO$				23.90 ± 0.12	3.28 ± 0.23	4.9×10^{-3} [c]
$MP2_gCM2$				20.47 ± 0.15	8.31 ± 0.24	1.3×10^{-6} [c]

[a] Free energy differences in kcal/mol. K(t/c): trans/cis equilibrium constants. [b] $T = 298.15$ K. [c] $T = 310$ K. [d] $T = 310$ K, free energy corrections calculated at $T = 298.15$ K.

the trans fraction in aqueous solution. Calculating, for example, the relative internal free energy by using the CCSD(T) internal energies by Tsai et al.,[4] the value of the $K(t/c)$ equilibrium constant (Table 9) increases to $4 \times 10^{-2} - 10^{-1}$ at $T = 310$ K.

In summary, calculations indicate that relative conformer energies and free energies are remarkably different for the $ONOO^-$ anion in aqueous solution. The small difference of these two thermodynamic characteristics for the cis−trans pair in the gas-phase is due to the small relative thermal correction: relative energies and free energies are 3.3 and 3.1 kcal/mol, respectively, at the B3LYP/6-311+G* level. In aqueous solution, the relative internal energy still remains 3.3 kcal/mol, whereas the relative trans free energy increases to 4.3 kcal/mol, as obtained with the continuum solvent method. In contrast, the calculated relative free energy is 1.8−2.5 kcal/mol if considering B3LYP calculated values from Monte Carlo simulations.

Solution Structure. Interpretation of the MC simulations with different solute geometries and charge parameterization leads to rather similar conclusions regarding both the structure of the first hydration shell around the solute and the solute−water hydrogen-bond pattern. Snapshots taken at the last configuration, using any simulation models, unanimously indicate that the O_4^- site is the most important site for hydrogen bonding with water, and the second most important site is the $=O_1$ site. Waters, even if they form hydrogen bonds to the O_3 and N atoms, are primarily bound to the O_4 and O_1 oxygens, respectively. Thus, the $O_1 \cdot\cdot H_2O$ and $O_4 \cdots H_2O$ hydrogen bonds will be more thoroughly analyzed in the present section.

Figure 4 shows $O_4^- \cdots H_w$ and $=O_1 \cdots H_w$ (water hydrogen) radial distribution functions (rdfs) obtained for the cis $ONOO^-$ with the $MP2_gELPO$ and $B3LYP_s$ models. Hydration of the anionic oxygen site is clearly indicated by high peaks, $g(R) = 4.03$ (MP2) and 3.54 (B3LYP) for the $O_4^- \cdots H_w$ rdfs at $R(O \cdot\cdot H) = 1.75$ Å. A well resolved second peak at 3.10 Å stems from the second, unbound hydrogens of the water molecules involved in hydrogen bonds to the solute. While these hydrogens are strongly located, they may not form a seven member ring with the $=O_1$ atom. Such a bifurcated structure was favorable in the monohydrate,[6] and could be also possible in the present case, where the $O_1 \cdots O_4^-$ distance is 2.4−2.5 Å. The $=O_1 \cdots H_w$ rdfs, however, do not show a resolved peak-structure in either case, suggesting that no stable hydrogen bonds are formed in aqueous solution at this site. Figures 5 and 6 with the $O_4^- \cdots H_w$ rdfs at the TS torsion angles and in the trans form, respectively, calculated with the $MP2_gELPO$, $MP2_gCM2$, and $B3LYP_s$ models show essential similarity to each other and to the cis $O_4^- \cdots H_w$ rdf in Figure 4. Thus, $O_4^- \cdots H_w$ rdfs provide high and narrow first peaks at about 1.75 Å, and a second, well resolved peak about 3.10 Å. Heights of the first peaks, g ($R = 1.75$), vary in the range of 3.5−5.1. Integration of the rdfs until the first minima provides 4.1−5.1 water hydrogens (Table 10),

TABLE 10: Calculated Statistical and Energy Terms Related to the Solution Structure[a]

	N (O_4^-/H_w) coordination numbers			number of hydrogen bonds (N_{HB}, $E_{int} \le -10$)		
	cis	TS	trans	cis	TS	trans
$B3LYP_s$	4.5	5.1	4.8	4.7	4.9	4.6
$MP2_gELPO$	4.9	4.7	4.4	4.9	5.0	4.1
$MP2_gCM2$	4.1	4.9	4.4	4.3	4.7	4.4
$B3LYP_{gs}$	4.3	4.9	4.2	4.3	4.5	4.0

	total hydrogen-bond energies			solute−solvent interaction energies		
	cis	TS	trans	cis	TS	trans
$B3LYP_s$	−62.1	−73.5	−64.2	−166	−179	−172
$MP2_gELPO$	−64.6	−65.8	−57.8	−167	−165	−172
$MP2_gCM2$	−61.4	−70.4	−57.7	−170	−176	−162
$B3LYP_{gs}$	−54.0	−62.2	−54.1	−155	−171	−163

	ΔH_{solv}		$T\Delta S_{solv}$	
	TS-cis	trans-cis	TS-cis	trans-cis
$B3LYP_s$	-5.9 ± 2.9	12.3 ± 4.6	2.1 ± 2.9	12.6 ± 4.6
$MP2_gELPO$	-11.6 ± 3.1	-12.3 ± 5.4	-11.1 ± 3.1	-12.2 ± 5.4
$MP2_gCM2$	18.4 ± 3.6	38.0 ± 5.7	22.4 ± 3.6	33.0 ± 5.7
$B3LYP_{gs}$	-2.0 ± 3.1	4.1 ± 5.0	2.8 ± 3.1	5.2 ± 5.0

[a] Energies in kcal/mol.

with a difference of up to 0.8 water molecules in the $N(O_4^-/H_w)$ coordination number for the first hydration shell of the O_4^- site in different conformations.

Pair-energy distribution functions (pedfs) obtained with different models at three torsion angles (Figures 7 and 8) show peaks at the most negative pair-interaction energy for the $B3LYP_s$ model (in-solution optimized geometry, atomic charges fitted to the polarized charge-distribution in solution). Pedfs have minima at $E = -11$ or -10 kcal/mol, and integrations of the curves up to the their minima give values in the range of 4.0−5.0, corresponding to the number of the hydrogen bonds (N_{HB}) to the solute with interaction energy in the -20 to -10 kcal/mol range. N_{HB} values in Table 10 differ only a little from the corresponding $N(O_4^-/H_w)$ coordination numbers, suggesting that the main contribution to the number of hydrogen bonds in the $E = -20$ to -10 kcal/mol range comes from the hydration of the O_4^- site. The relationship $N(O_4^-/H_w) < N_{HB}$ indicates hydrogen bonds also at sites other than at O_4^-, whereas $N(O_4^-/H_w) > N_{HB}$ means that not all water molecules in the first hydration shell form hydrogen bonds to O_4^-.

Onset of the rise of the pedfs for the cis conformer around -19 kcal/mol allows an important conclusion concerning the quality of the charge parameterization. From the study of Tsai et al.,[6] the monohydrate binding energy at the MP2/6-311+G* level is -17.0 to -17.8 kcal/mol at the primary binding site of the cis $ONOO^-$. The interaction energy of the solute and *one*

solvent molecule obtained with a 12−6−1 effective pair potential in MC simulations is the counterpart of the monohydrate binding energy from ab initio calculations. Due to thermal motion, it is almost impossible to observe a solute−solvent pair-interaction energy equal to the theoretically lowest possible value. Thus, pedfs should start at a less negative value than the theoretical limit, −17.8 kcal/mol in this case. The accepted solute charges in the BOSS program should mimic, however, a solute polarized by *many* solvents, and the TIP4P parameters represent a solvent molecule polarized in bulk water. Then the pair-interaction energy should be more negative than the quantum-chemically calculated value, and the threshold value shifts *below* the monohydrate binding energy. The threshold lowering by about 1−2 kcal/mol reflects a reasonable shift as a balance of the thermal disordering and the more negative interaction energy between a polarized solute and a polarized solvent molecule. The pedf starts rising in the range of −18 to −17 kcal/mol for the trans form. Since the lowest monohydrate binding energy was calculated at −17.7 kcal/mol for the trans form, the present parameterization does not result in a lowering of the threshold value, which would be, however, desired based on the above argument.

Pedfs for the TS and trans conformers generally show a shoulder between $E = -10$ and −7 kcal/mol. This finding suggests a gradually developing second hydration site for these conformers, which is independent of the O_4^- hydration and has not been accounted for by the N_{HB} values in Table 10. Indeed, $=O_1\cdots H_w$ rdfs for the trans $ONOO^-$ show well-resolved peaks at about 1.85 Å, and a value of 2.5 has been derived with the $B3LYP_s$ model for the $N(=O_1/H_w)$ coordination number. The corresponding number of hydrogen bonds, calculated from the integration of pedf in Figure 8 within the range of $E = -10$ to −7 kcal/mol, is 2.8, almost equal to the $N(=O_1/H_w)$ coordination number. Molecules in this energy range should correspond to those located around the $=O_1$ site.

The N_{HB} numbers are generally only slightly larger for the TS than for the cis and trans conformers, whereas the solvation free energy profiles in Table 8 differ considerably for the different models. Instead of considering N_{HB}, total hydrogen bond interaction energies calculated by numerical integration of the $E \times (dN(E)/dE)$ product in the −20 to −10 kcal/mol interaction energy range show remarkable differences (Table 10). In this data set, the TS value is clearly the most negative one and is remarkably more negative than that for the cis and trans conformers both with the $B3LYP_s$ and $B3LYP_{gs}$ models. Although the interaction energies with charge sets derived in the gas-phase ($B3LYP_{gs}$) are smaller than those from the $B3LYP_s$ simulations, the differences in the hydrogen-bond energies for the TS−cis as well as for the trans−cis pairs are similar using the two models, and provide a rationale for the similarity of the ΔG(solv) curves.

Finally, one more question can be raised: why and how is the TS structure stabilized by solvent effects in the Monte Carlo simulations? On the basis of rdfs, the solution structure shows only fine differences. Total hydrogen bond interaction energies (up to $E = -10$ kcal/mol) are 33−41% of the entire solute−solvent interaction energies (Table 10) but do not follow the pattern and relative values of the ΔG(solv) curves. A partitioning of the ΔG(solv) value into ΔH_{solv} and $T\Delta S_{solv}$ contributions can be performed only with large uncertainty from Monte Carlo simulations calculating ΔG(solv) by FEP. Since $\Delta G(solv) = \Delta H_{solv} - T\Delta S_{solv}$, both the solvation enthalpy and entropy are favorable for the cis to TS conformational change at the B3LYP level. With the $MP2_g$ELPO model the two effects almost cancel each other, whereas the process is entropy driven from $MP2_g$-CM2 simulations. For the trans form, the approximate enthalpy−entropy cancellation is well demonstrated (with the exception of $MP2_g$CM2 simulations), but the very different ΔH_{solv} terms emphasize again the sensitivity of the solvation results to the charge parameterization. Thus, only the ΔG(solv) term, but not its components, should be taken with significance (in fact, ΔG(solv) was obtained directly upon the free energy perturbation method, while ΔH_{solv} was obtained from a less effective calculation with umbrella sampling). The ΔG(solv) results are fairly consistent, providing solvation free energy for the trans conformer of −1.2 to −0.1 kcal/mol relative to the cis form with the three best models.

Summary

Gas-phase calculations at the B3LYP/6-311+G* and MP2/6-311+G* levels predict free energies of 3.1 kcal/mol ($T = 298.15$) and 3.4 kcal/mol ($T = 310$), respectively, for the trans conformer relative to the cis form for peroxynitrite anion. The aqueous environment increases the relative stability of the cis conformation as calculated with the SCI−PCM method at the B3LYP/6-311+G* level. The cis−trans relative internal energy hardly changes as compared to its gas-phase value. The only remarkable contribution to ΔG(solv) comes from the solute−solvent interaction energy term (1.3 kcal/mol), resulting in an overall stability of 4.3 kcal/mol for the cis form in aqueous solution.

The opposite trend has been found by combined (ab initio or DFT)/Monte Carlo simulations at the B3LYP/6-311+G* and MP2/6-311+G* levels. B3LYP/6-311+G*/MC calculations predict a decrease of the relative free energy to 1.8−2.5 kcal/mol at the temperature of $T = 310$ K in humans. $MP2_g$ELPO simulations do not show remarkable solvent effects on the cis−trans free energy separation. None of the present results contradicts the interpretation of the experimental Raman spectrum of $ONOO^-$ by Tsai et al.[5] in favor of the cis form, but calls the attention to the different trends at the B3LYP/6-311+G* level when using the SCI−PCM continuum solvent and Monte Carlo explicit solvent methods.

All calculations indicate the lowering of the free energy for the barrier at $\tau = 77°-80°$. Continuum-dielectric calculations show a decrease of the barrier by 1.8 kcal/mol upon solvation. The barrier decreases by up to 7 kcal/mol and has been predicted as 18−24 kcal/mol on the basis of B3LYP and MP2/Monte Carlo simulations.

Monte Carlo simulations find about five strong hydrogen bonds to the O_4^- site in any conformations. The second strongest hydration site is the $=O_1$ atom forming 2−3 weaker hydrogen bonds mainly in the trans $ONOO^-$ conformation. Both enthalpy and entropy are favorable at the B3LYP level in stabilizing the TS structure, whereas the calculated small relative solvent effect for the trans form is the consequence of the enthalpy−entropy cancellation. Overall, this study suggests that a combined (ab initio or DFT/Monte Carlo) type calculation is a powerful method in calculating solute thermodynamics and solution structure, if the solute geometry is previously optimized using a continuum method, the atomic charges are fitted to a correlated and in-solution polarized charge distribution, and thermal corrections are calculated even from gas-phase results.

Acknowledgment. The author thanks the Ohio Supercomputer Center for the computer time used in the quantum chemical calculations. He also thanks Professor Jorgensen for the use of the BOSS 3.6 program.

References and Notes

(1) (a) Beckman, J. S.; Beckman, T. W.; Chen, J.; Marshall, P. A.; Freeman, B. A. *Proc. Natl. Acad. Sci. U.S.A.* **1990**, *87*, 1620. (b) Beckman, J. S.; Koppenol, W. H. *Am. J. Physiol.* **1996**, *271*, 1424.

(2) For a recent review, see Szabo, C. In *Recent Advances in Nitric Oxide Research*, Kitabataka, A., Sakuma, I., Eds.; Springer-Verlag: Tokyo, 1999; pp 1−20.

(3) Koppenol, W. H.; Kissner, R. *Chem. Res. Toxicol.* **1998**, *11*, 87.

(4) Tsai, H.-H.; Hamilton, T. P.; Tsai, J.-H. M.; Van der Woerd, M.; Harrison, J. G.; Jablonsky, M. J.; Beckman, J. S.; Koppenol, W. H. *J. Phys. Chem.* **1996**, *100*, 15087.

(5) Tsai, J.-H. M.; Harrison, J. G.; Martin, J. C.; Hamilton, T. P.; Van der Woerd, M.; Jablonsky, M. J.; Beckman, J. S. *J. Am. Chem. Soc.* **1994**, *116*, 4115.

(6) Tsai, H.-H.; Hamilton, T. P.; Tsai, J.-H. M.; Beckman, J. S.; Koppenol, W. H. *Struct. Chem.* **1995**, *6*, 323.

(7) Doclo, K.; Rothlisberger, U. *J. Phys. Chem. A* **2000**, *104*, 6464.

(8) (a) Foresman, J. B.; Keith, T. A.; Wiberg, K. B.; Snoonian, J.; Frisch, M. J. *J. Phys. Chem.* **1996**, *100*, 16098. (b) *CRC Handbook of Chemistry and Physics*, 81st edition; CRC Press LLC: Boca Raton, FL.

(9) Tomasi, J.; Persico, M. *Chem. Rev.* **1994**, *94*, 2027.

(10) (a) Miertuš, S.; Scrocco, E.; Tomasi, J. *Chem. Phys.* **1981**, *55*, 117. (b) Miertuš, S.; Tomasi, J. *Chem. Phys.* **1982**, *65*, 239.

(11) Orozco, M.; Luque, F. J.; Habibollahzadeh, D.; Gao, J. *J. Chem. Phys.* **1995**, *102*, 6145.

(12) McQuerrie, D. *Molecular Mechanics*; Harper and Row: New York, 1976.

(13) Hehre, W. J.; Radom, L.; Schleyer, P. v. R.; Pople, J. A. *Ab Initio Molecular Orbital Theory*; Wiley: New York, 1986.

(14) (a) Lee, C.; Yang, W.; Parr, R. G. *Phys. Rev. B* **1988**, *37*, 785. (b) Becke, A. D. *J. Chem. Phys.* **1993**, *98*, 5648.

(15) Frisch, M. J.; Trucks, G. W.; Schlegel, H. B.; Scuseria, G. E.; Robb, M. A.; Cheeseman, J. R.; Zakrzewski, V. G.; Montgomery, J. A., Jr..; Stratmann, R. E.; Burant, J. C.; Dapprich, S.; Millam, J. M.; Daniels, A. D.; Kudin, K. N.; Strain, M. C.; Farkas, O.; Tomasi, J.; Barone, V.; Cossi, M.; Cammi, R.; Mennucci, B.; Pomelli, C.; Adamo, C.; Clifford, S.; Ochterski, J.; Petersson, G. A.; Ayala, P. Y.; Cui, Q.; Morokuma, K.; Malick, D. K.; Rabuck, A. D.; Raghavachari, K.; Foresman, J. B.; Cioslowski, J.; Ortiz, J. V.; Stefanov, B. B.; Liu, G.; Liashenko, A.; Piskorz, P.; Komaromi, I.; Gomperts, R.; Martin, R. L.; Fox, D. J.; Keith, T.; Al-Laham, M. A.; Peng, C. Y.; Nanayakkara, A.; Gonzalez, C.; Challacombe, M.; Gill, P. M. W.; Johnson, B.; Chen, W.; Wong, M. W.; Andres, J. L.; Gonzalez, C.; Head-Gordon, M.; Replogle, E. S.; Pople, J. A. *Gaussian 98*, rev. A.6.; Gaussian, Inc.: Pittsburgh, PA, 1998.

(16) Floris, F. M.; Tomasi, J. *J. Comput. Chem.* **1991**, *12*, 784.

(17) (a) Pierotti, R. A. *J. Phys. Chem.* **1963**, *67*, 1840. (b) Pierotti, R. A. *J. Phys. Chem.* **1965**, *69*, 281.

(18) Claverie, P.; Daudey, J. P.; Langlet, J.; Pullman, B.; Piazzola, D.; Huron, M. J. *J. Phys. Chem.* **1978**, *82*, 405.

(19) (a) Jorgensen, W. L.; Madura, J. D. *J. Am. Chem. Soc.* **1983**, *105*, 1407. (b) Jorgensen, W. L.; Swenson, C. J. *J. Am. Chem. Soc.* **1985**, *107*, 1489. (c) Jorgensen, W. L.; Gao, J. *J. Phys. Chem.* **1986**, *90*, 2174. (d) Jorgensen, W. L.; Briggs, J. M.; Contreras, M. L. *J. Phys. Chem.* **1990**, *94*, 1683.

(20) (a) Jorgensen, W. L. BOSS, Version 3.6, *Biochemical and Organic Simulation System User's Manual*; Yale University: New Haven, CT, 1995.

(21) (a) Jorgensen, W. L.; Chandrasekhar, J.; Madura, J. D.; Impey, R. W.; Klein, M. L. *J. Chem. Phys.* **1983**, *79*, 926. (b) Jorgensen, W. L.; Madura, J. D. *Mol. Phys.* **1985**, *56*, 1381.

(22) Jorgensen, W. L.; Tirado-Rives, J. *J. Am. Chem. Soc.* **1988**, *110*, 1657.

(23) (a) Carlson, H. A.; Nguyen, T. B.; Orozco, M.; Jorgensen, W. L. *J. Comput. Chem.* **1993**, *14*, 1240. (b) Orozco, M.; Jorgensen, W. L.; Luque, F. J. *J. Comput. Chem.* **1993**, *14*, 1498.

(24) Breneman, C. M.; Wiberg, K. B. *J. Comput. Chem.* **1990**, *11*, 316.

(25) Nagy, P. I.; Takács-Novák, K. *J. Am. Chem. Soc.* **2000**, *122*, 6583.

(26) Li, J.; Zhu, T.; Cramer, C. J.; Truhlar, D. G. *J. Phys. Chem. A* **1998**, *102*, 1820.

(27) AMSOL-version 6.6. Hawkins, G. D.; Giesen, D. J.; Lynch, G. C.; Chambers, C. C.; Rossi, I.; Storer, J. W.; Li, J.; Winget, P.; Rinaldi, D.; Liotard, D. A.; Cramer, C. J., and Truhlar, D. G. University of Minnesota, 1999.

(28) Dewar, M. J. S.; Zoebisch, E. G.; Healy, E. F.; Stewart, J. J. P. *J. Am. Chem. Soc.* **1988**, *110*, 1657.

(29) Stewart, J. J. P. *J. Comput. Chem.* **1989**, *10*, 209.

(30) Zwanzig, *J. Chem. Phys*. **1954**, *22*, 1420.

(31) Jorgensen, W. L.; Ravimohan, C. *J. Chem. Phys.* **1985**, *83*, 3050.

(32) Böttcher, C. J. F. *Theory of Electric Polarisation*; Elsevier: Amsterdam, 1952.

(33) Neumann, M. *J. Chem. Phys.* **1986**, *85*, 1567.

(34) Onsager, L. *J. Am. Chem. Soc.* **1936**, *58*, 1486.

(35) Nagy, P. I.; Durant, J. G.; Hoss, W. P.; Smith, D. A. *J. Am. Chem. Soc.* **1994**, *116*, 4898, 7957.

(36) Nagy, P. I., Alagona, G.; Ghio, C. *J. Am. Chem. Soc.* **1999**, *121*, 4804.

(37) (a) Nagy, P. I.; Flock, M.; Ramek, M. *J. Phys. Chem. A* **1997**, *101*, 5942. (b) Ramek, M.; Nagy, P. I. *J. Phys. Chem. A* **2000**, *104*, 6844. (c) Nagy, P. I.; Takács-Novák, K.; Ramek, M. *J. Phys. Chem. B* **2001**, *105*, 5772.

(38) Nagy, P. I.; Alagona, G.; Ghio, C., in preparation.

(39) (a) Nagy, P. I.; Takács-Novák, K. *J. Am. Chem. Soc.* **1997**, *119*, 4999. (b) Nagy, P. I.; Noszál, B. *J. Phys. Chem. A* **2000**, *104*, 6834.

(40) (a) Nagy, P. I.; Dunn, W. J., III.; Alagona, G.; Ghio, C. *J. Phys. Chem.* **1993**, *97*, 4628. (b) Nagy, P. I.; Durant, J. G. *J. Chem. Phys.* **1996**, *104*, 1452. (c) Alagona, G.; Ghio, C.; Nagy, P. I.; Durant, J. G. *J. Phys. Chem. A* **1999**, *103*, 1857.